Electronic Supplementary Material (ESI) for Nanoscale.

Supplementary Information

Luminescence Switching of Polymerically Confined Carbon Nanoparticles Triggered by UV-light

Indrajit Srivastava,[a,b] Parikshit Moitra,[d] Dinabandhu Sar,[a,b] Kevin Wang,[a,b] Maha Alafeef,[a,b,d,e,f] John Scott,[c] Dipanjan Pan[a,b,c,d,e*]

[a] Departments of Bioengineering, Materials Science and Engineering, Beckman Institute for Advanced Science and Technology, and Cancer Center at Illinois, University of Illinois at Urbana-Champaign, Urbana, IL, 61801, USA

[b] Mills Breast Cancer Institute, Carle Foundation Hospital, Urbana, IL, 61801, USA

[c] Illinois Sustainable Technology Center, University of Illinois at Urbana-Champaign, Champaign, IL, 61820, USA

[d] Departments of Diagnostic Radiology and Nuclear Medicine and Pediatrics, University of Maryland Baltimore, Health Sciences Facility III,670WBaltimoreSt., Baltimore, Maryland, 21201, USA

[e] Department of Chemical, Biochemical and Environmental Engineering, University of Maryland Baltimore County, Interdisciplinary Health Sciences Facility,1000 Hilltop Circle Baltimore, Maryland, 21250, USA

[f] Department of Biomedical Engineering, Faculty of Engineering, Jordan University of Science and Technology, Irbid, Jordan

Email: dipanjan@som.umaryland.edu

S. No.	Table of contents	Pg. No.

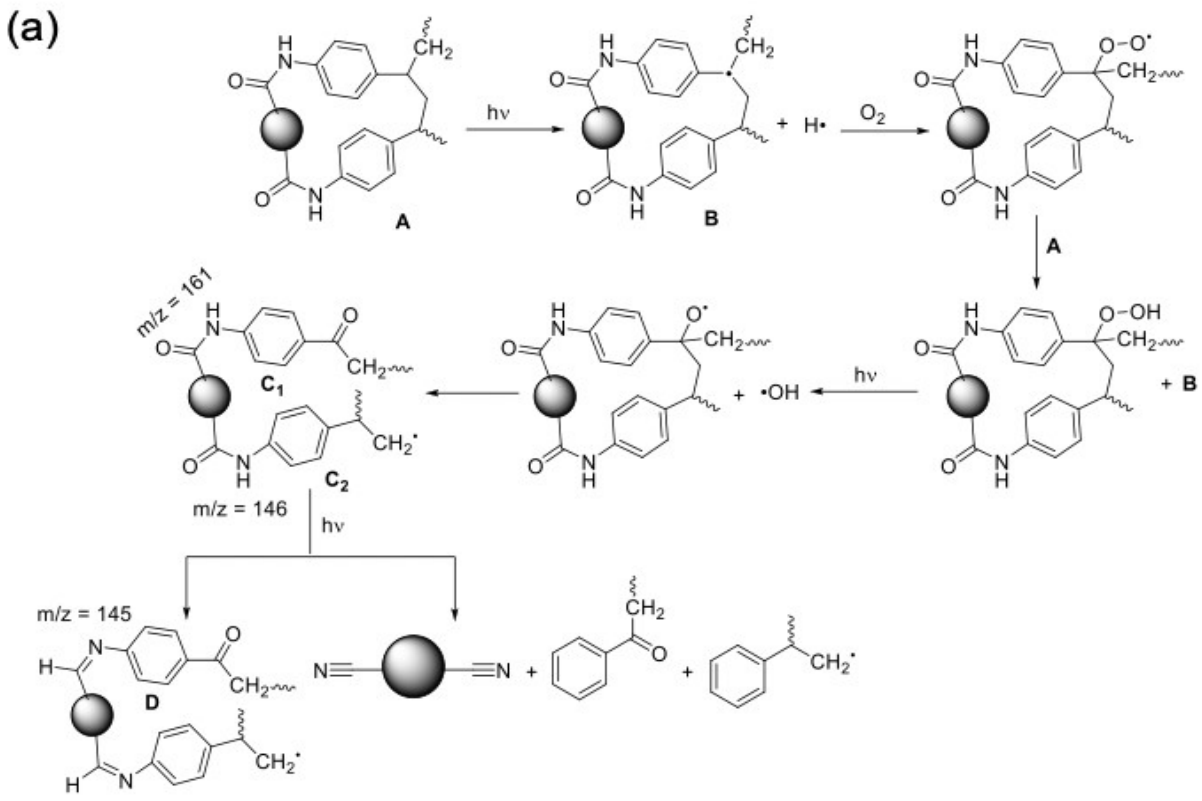

Scheme S1. Mechanism of CNP-PS degraded by UV-light irradiation.

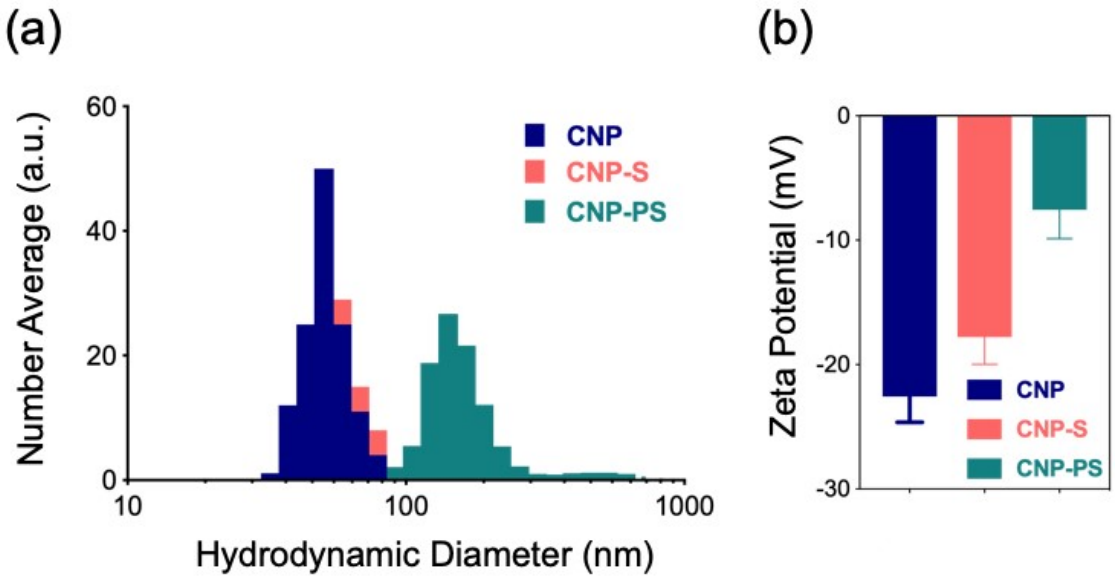

Figure S1. Hydrodynamic diameter measurements *via* DLS and (b) Zeta potential measurements for CNP, CNP-S and CNP-PS.

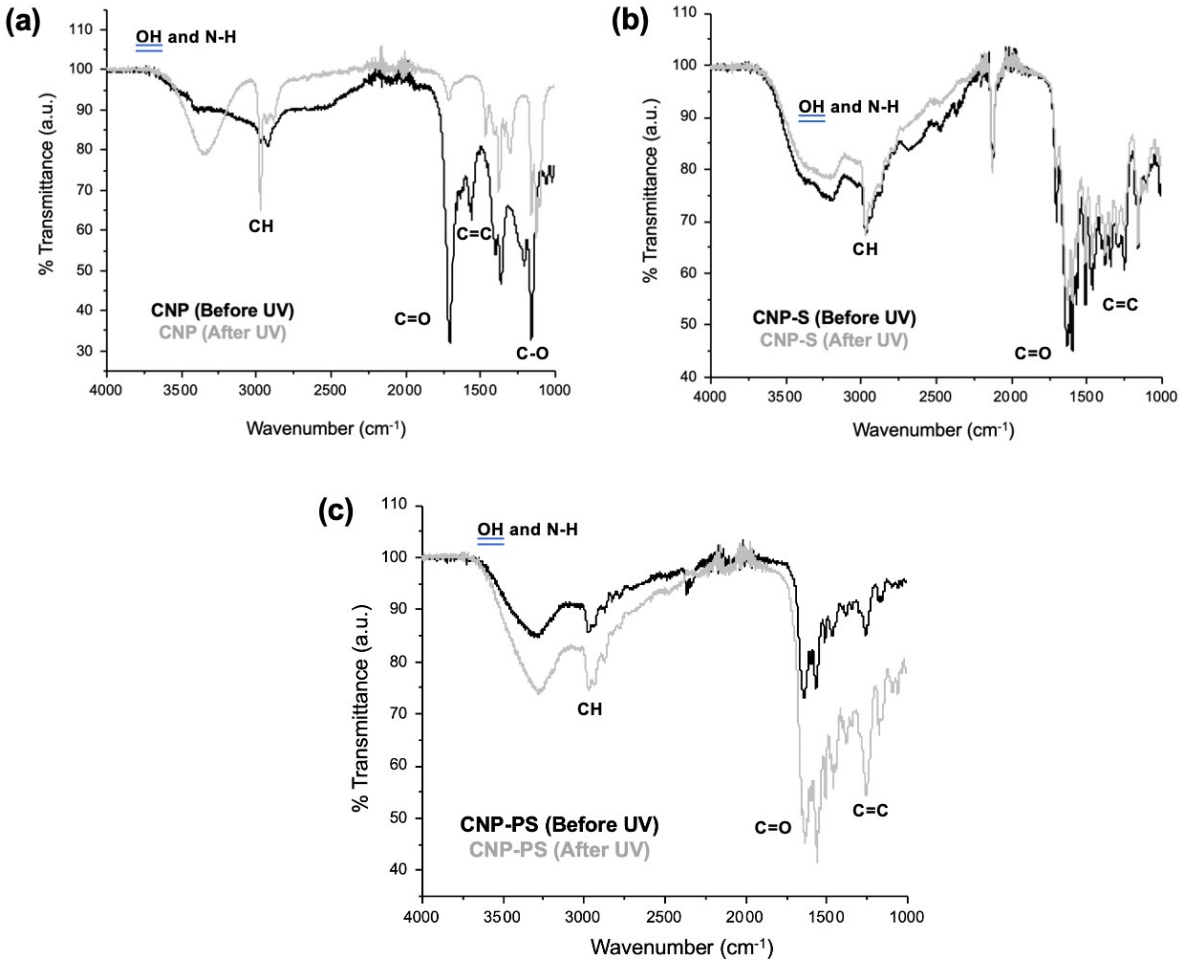

Figure S2. Fourier-transform infrared spectroscopy (FT-IR) measurement before and after UV light irradiation for (a) as-synthesized CNP, (b) CNP-S, and (c) CNP-PS.

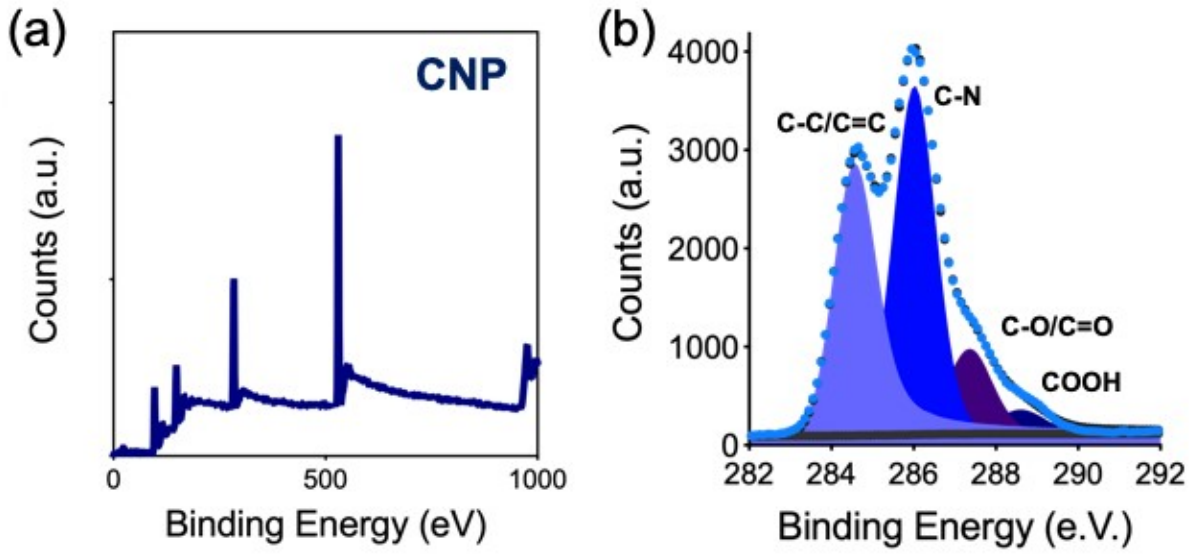

Figure S3. (a) X-Ray photoelectron spectra (XPS) of CNP, with high-resolution C1s (b) provided and de-convolved based on the literature.

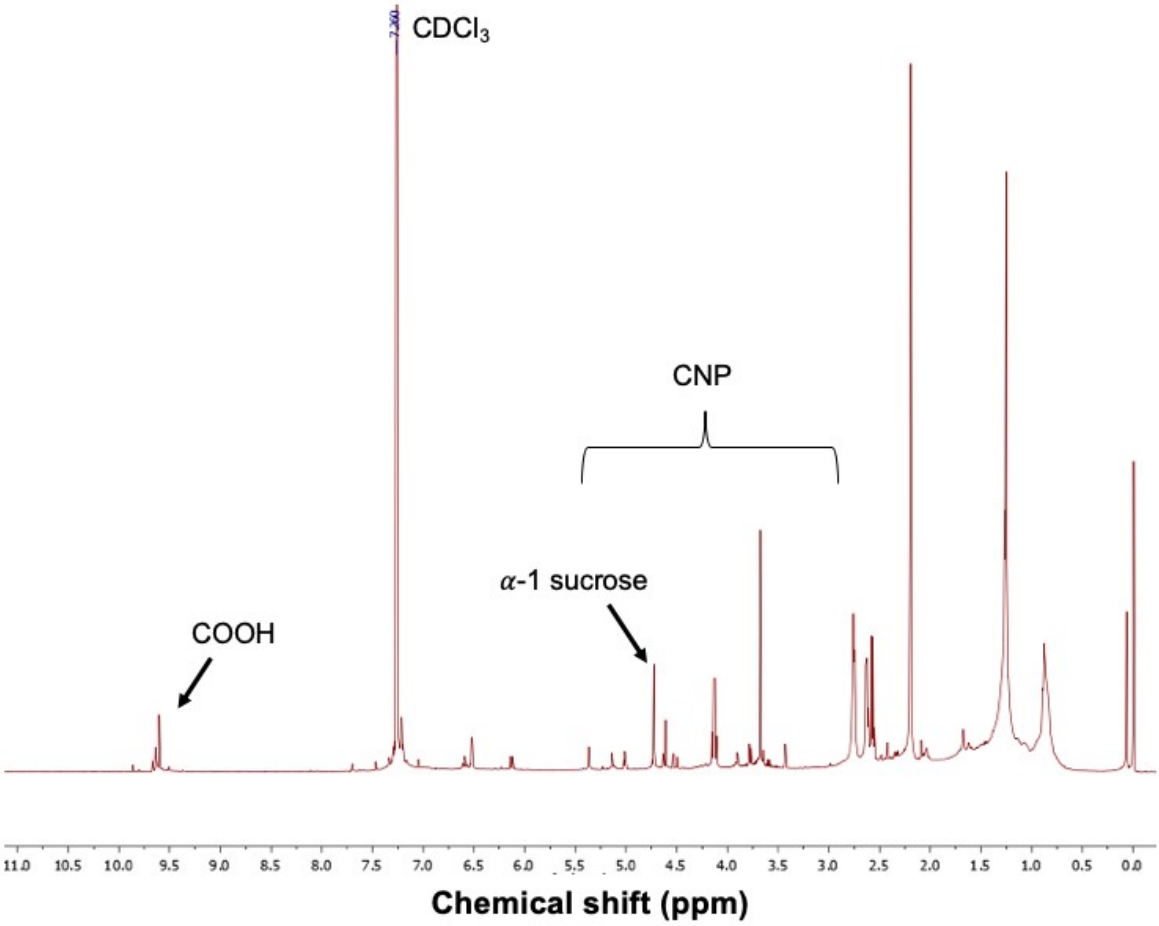

Figure S4. ^{1}H NMR Spectra of CNP.

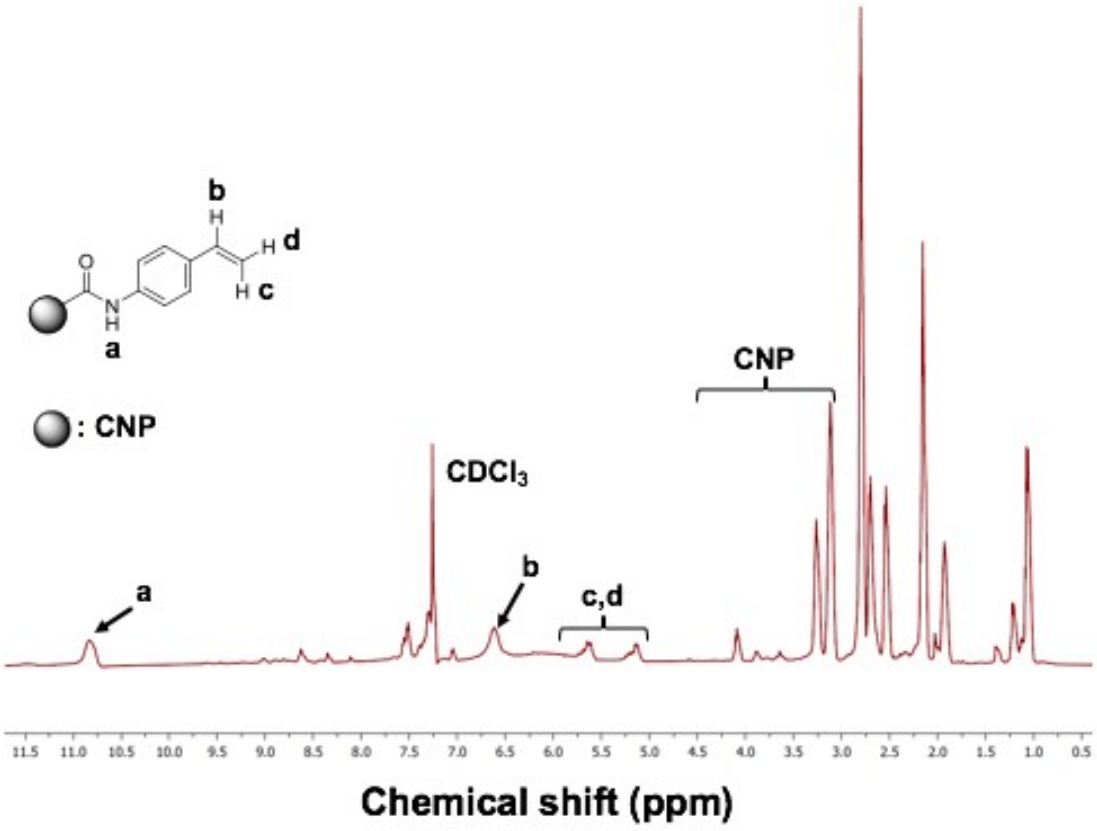

Figure S5. ^{1}H NMR Spectra of CNP-S showing successful chemical conjugation of 4-vinyl aniline (S) via carbodiimide chemistry.

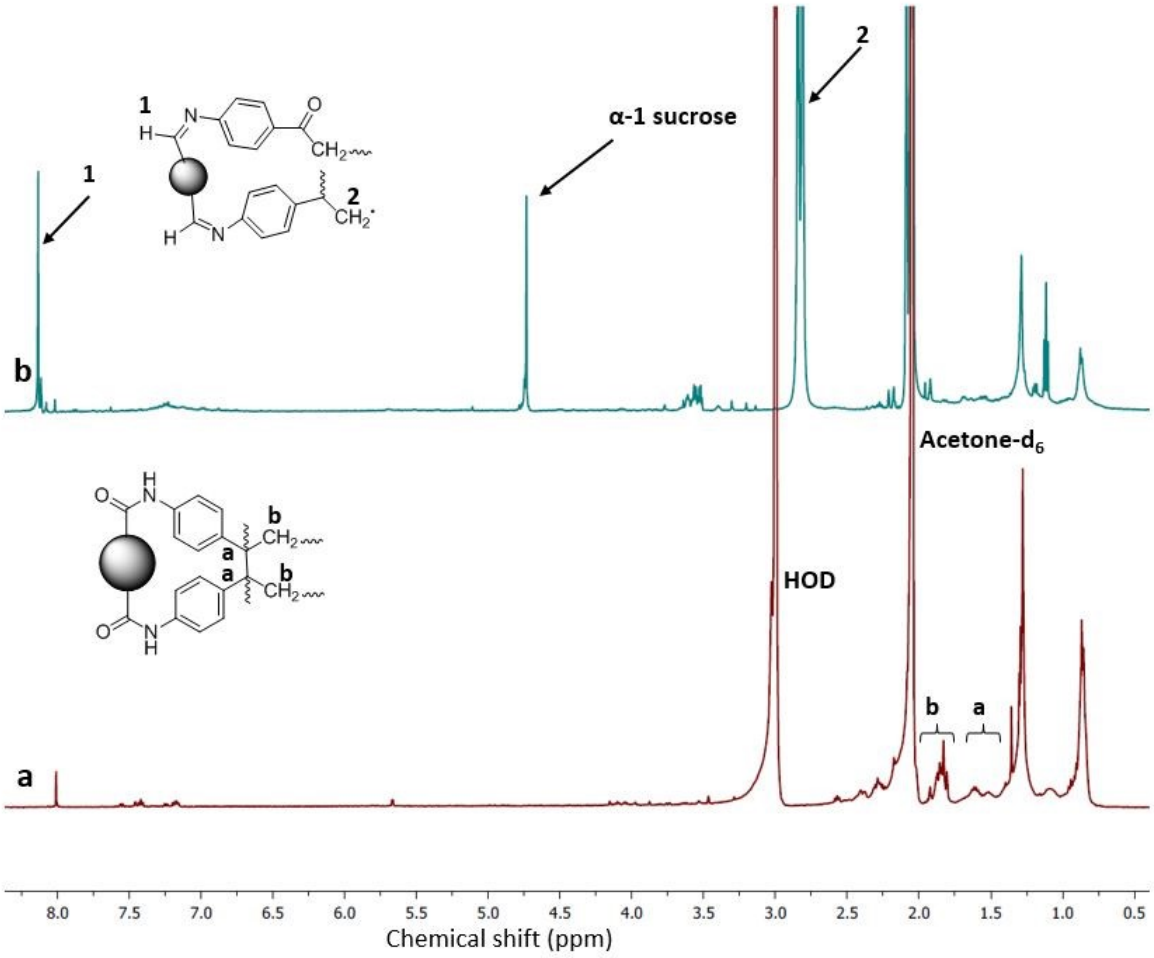

Figure S6. ^{1}H NMR Spectra of **(a)** CNP-PS showing successful polymerization at the nanoscale surface and **(b)** CNP-PS irradiated with UV light for 24h.

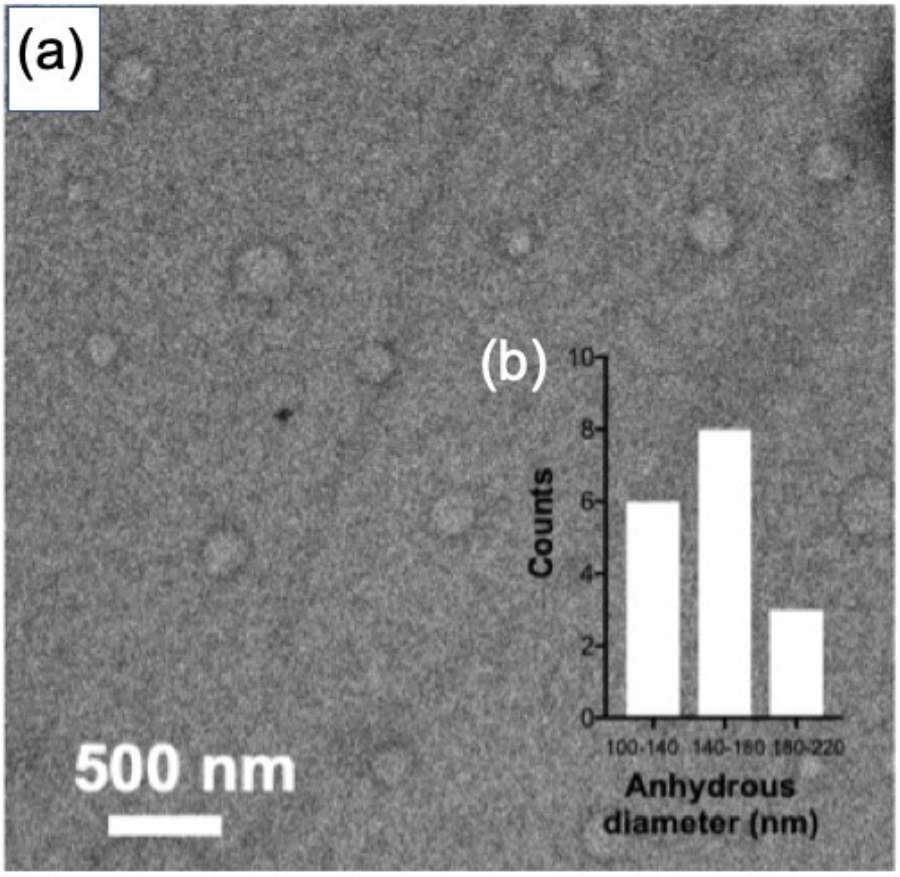

Figure S7. Transmission electron microscopy (TEM) image for CNP-PS (a) with anhydrous diameter calculations (b).

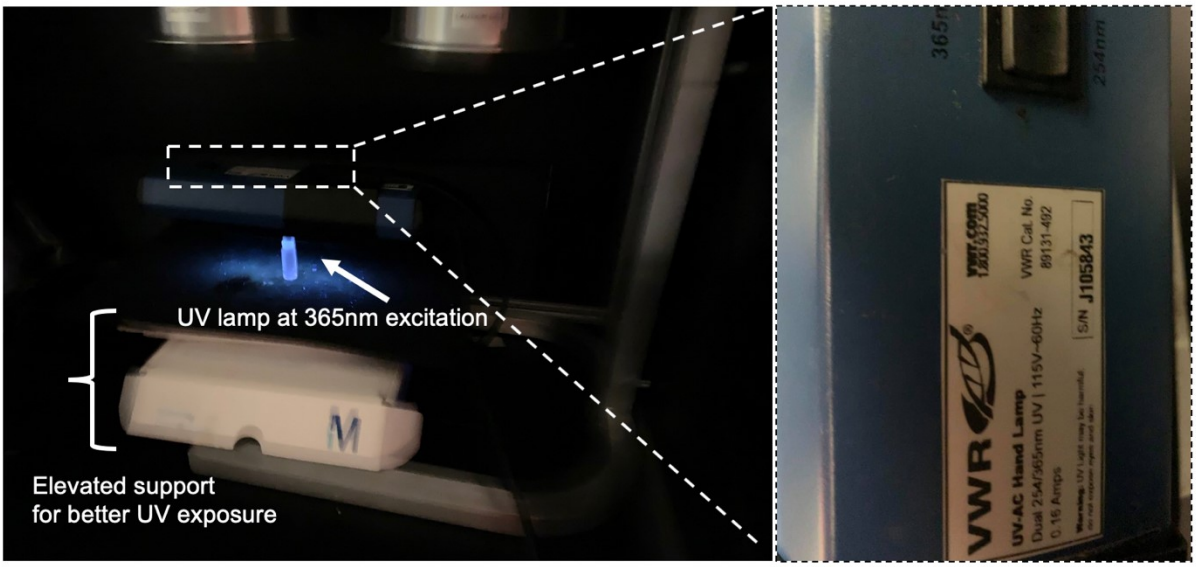

Figure S8. Experimental setup to perform the UV light irradiation on different CNP samples.

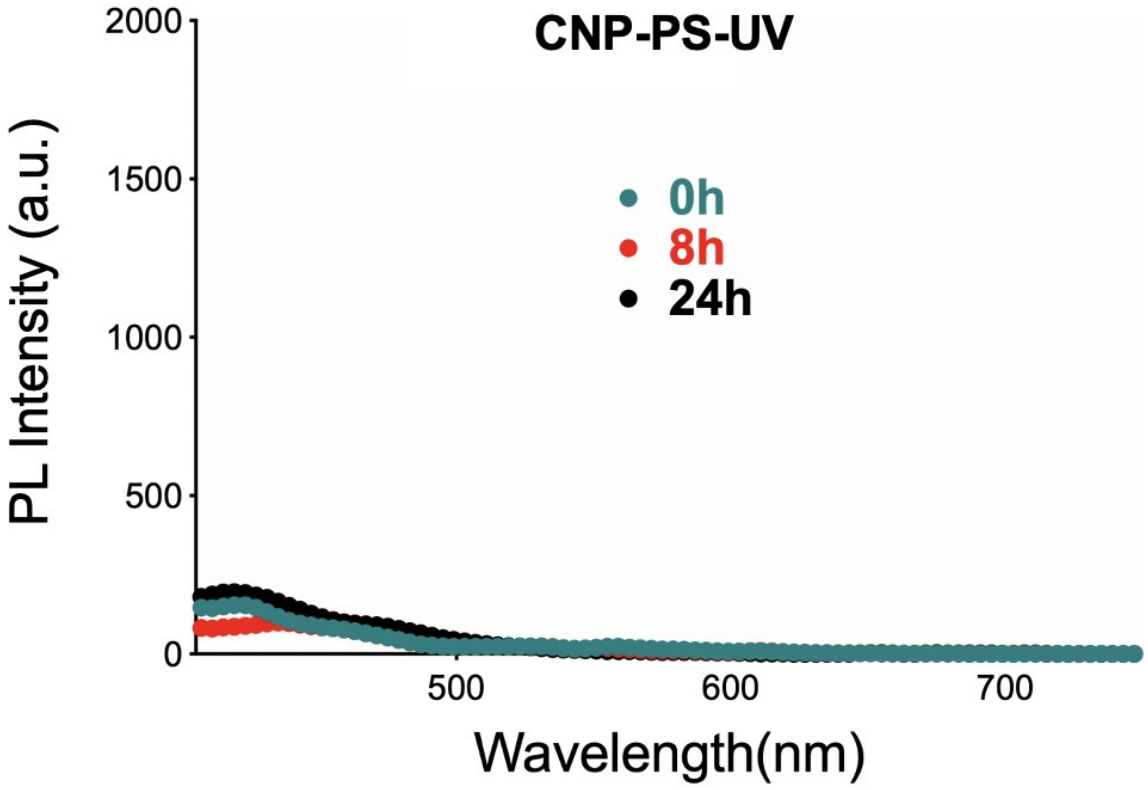

Figure S9. PL emission spectra of CNP-PS at t =0h, 8h and 24h, respectively kept under room temperature with no UV light exposure.

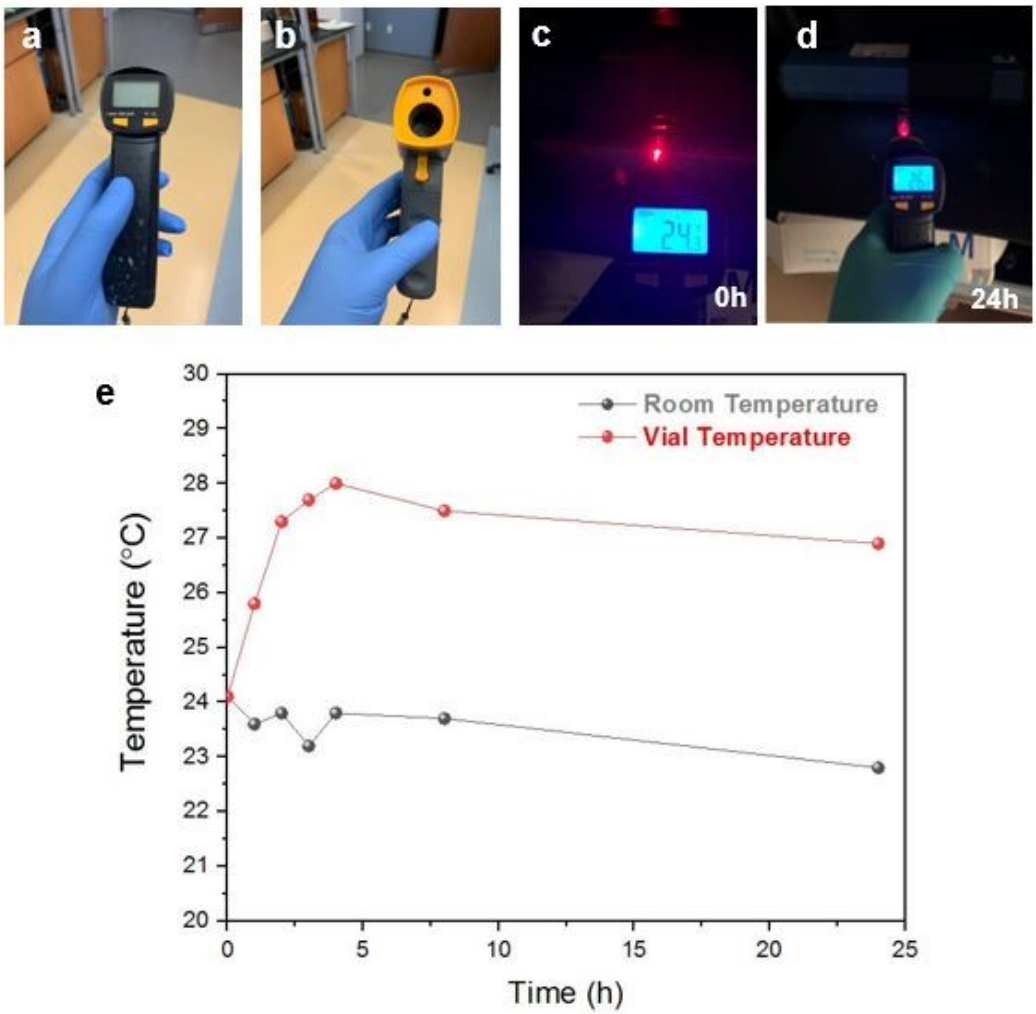

Figure S10. Monitoring the temperature of the vial using a non-contact infrared thermometer (a, b). Images taken at 0h (c) and 24h (d) by pointing the infrared laser onto the vial kept under the UV setup. (e) Subsequent temperature recordings for both the room temperature and vial temperature we collected at 0h, 1h, 2h, 3h, 4h, 8h, and 24h.

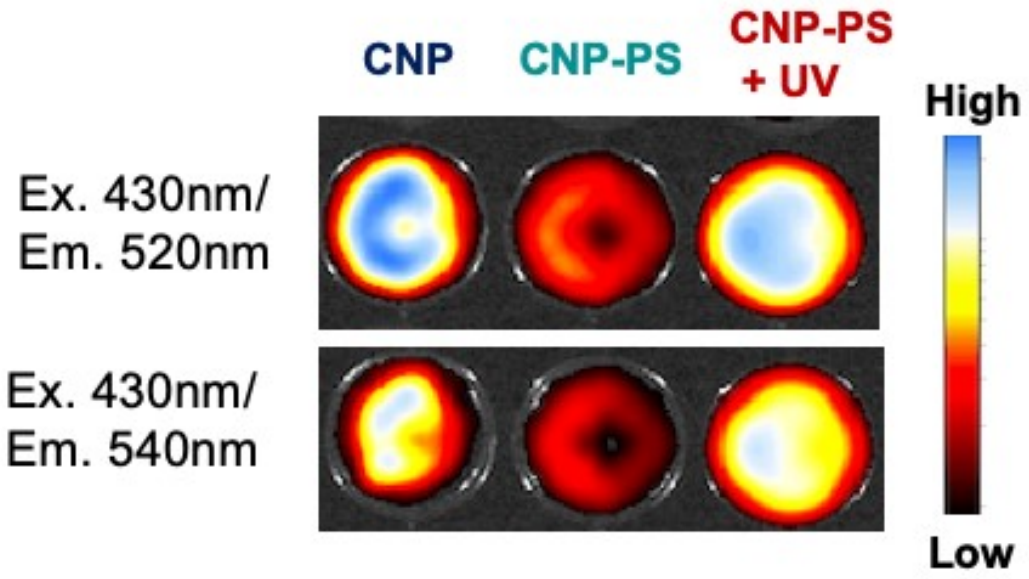

Figure S11. Fluorescence imaging signals for different samples obtained via IVIS under excitation wavelength of 465nm and emission filters at 520nm and 540nm.

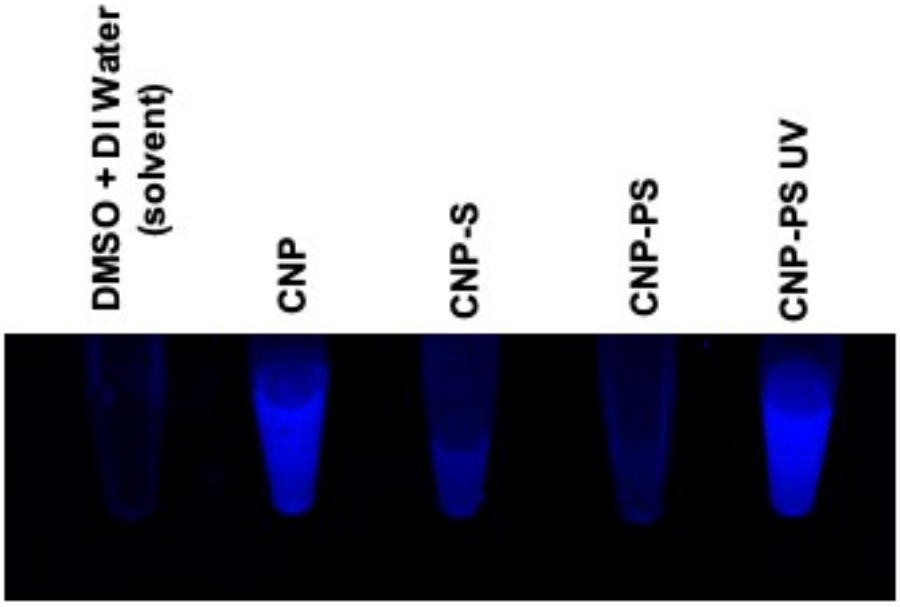

Figure S12. Gel dock luminescence images obtained for different samples under 530nm emission.

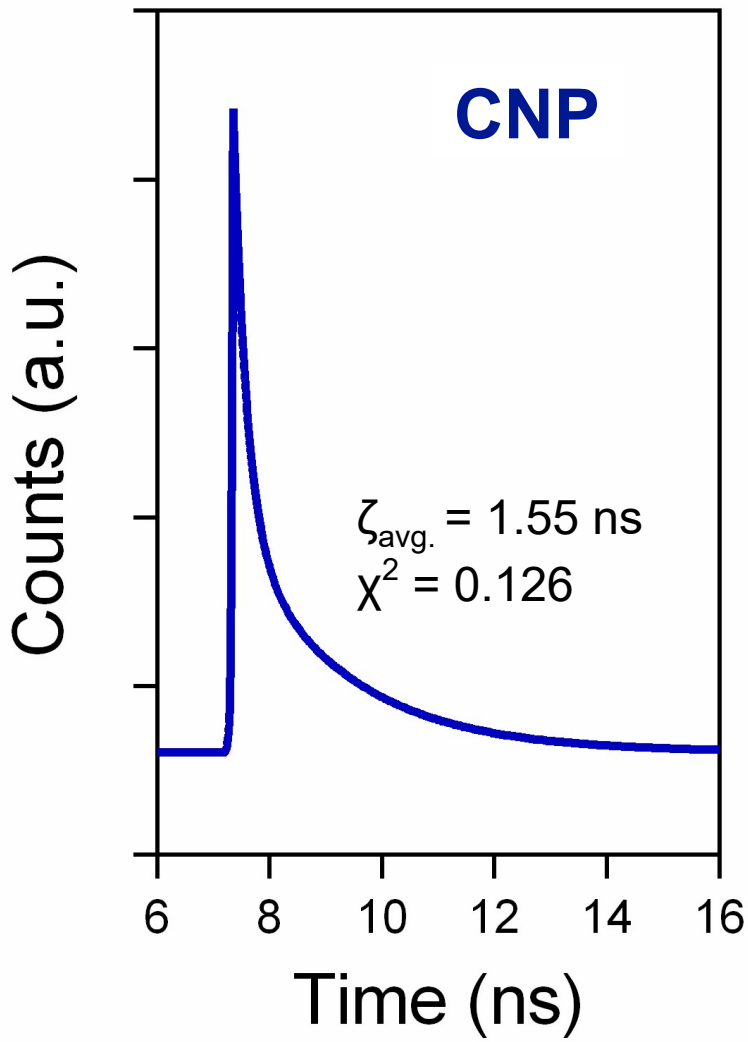

Figure S13. Time-resolved photoluminescence spectra of CNP at excitation wavelength of 390nm.

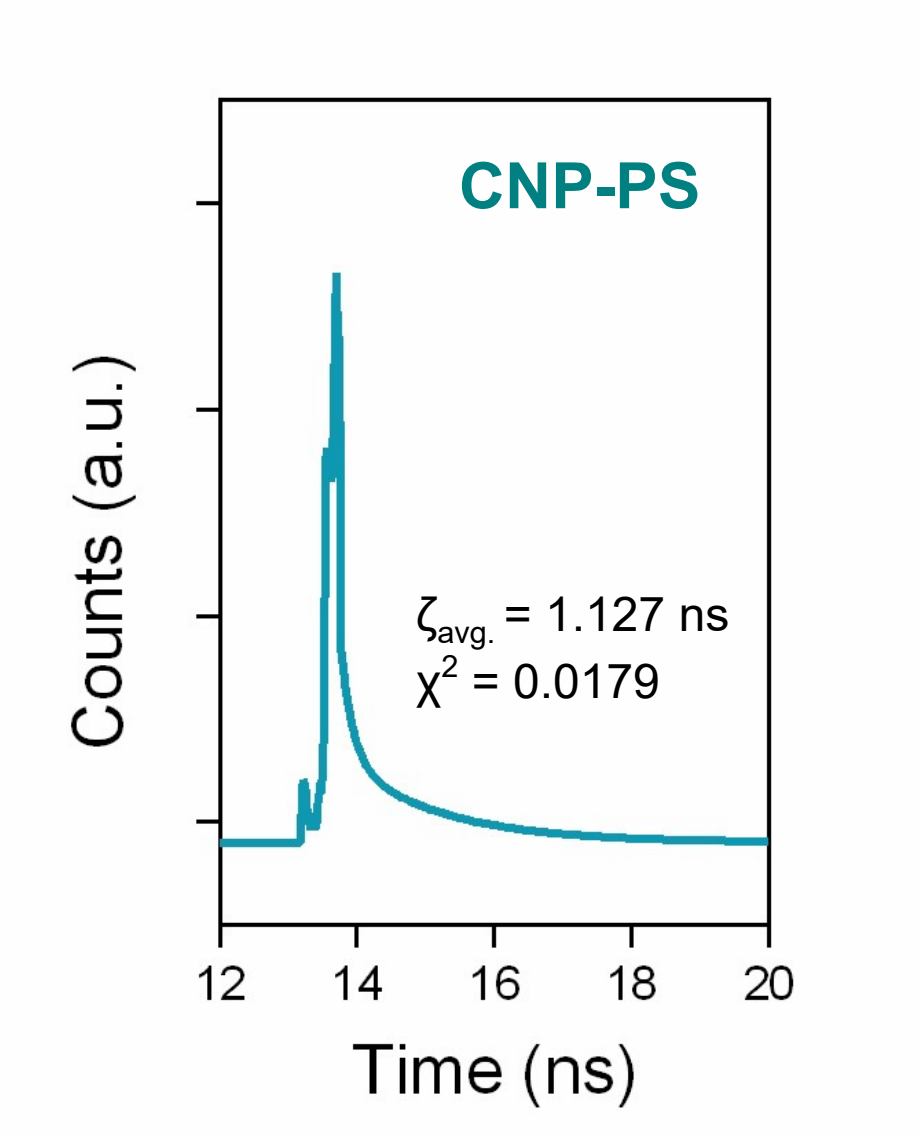

Figure S14. Time-resolved photoluminescence spectra of CNP-PS at excitation wavelength of 390nm.

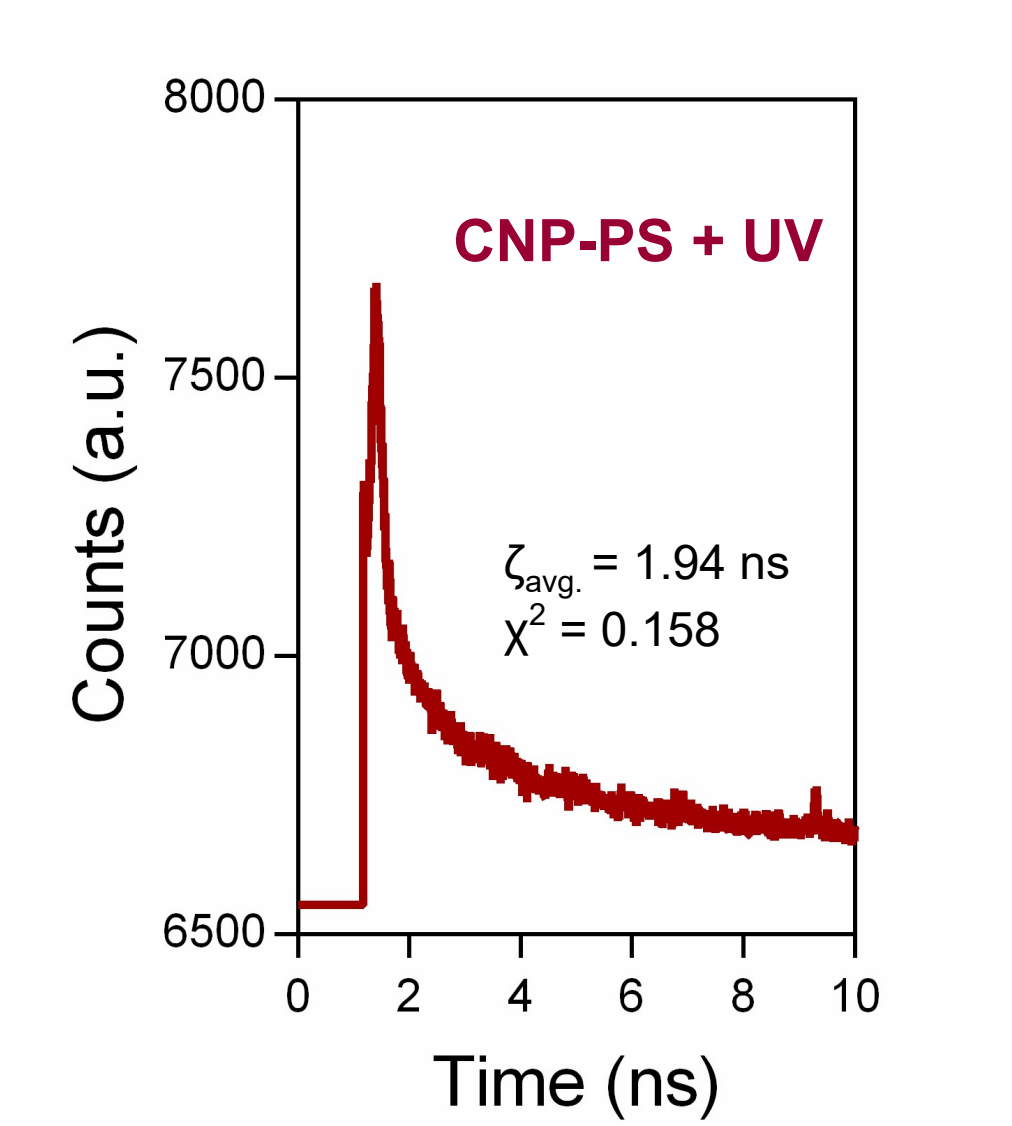

Figure S15. Time-resolved photoluminescence spectra of CNP-PS+UV at excitation wavelength of 390nm.

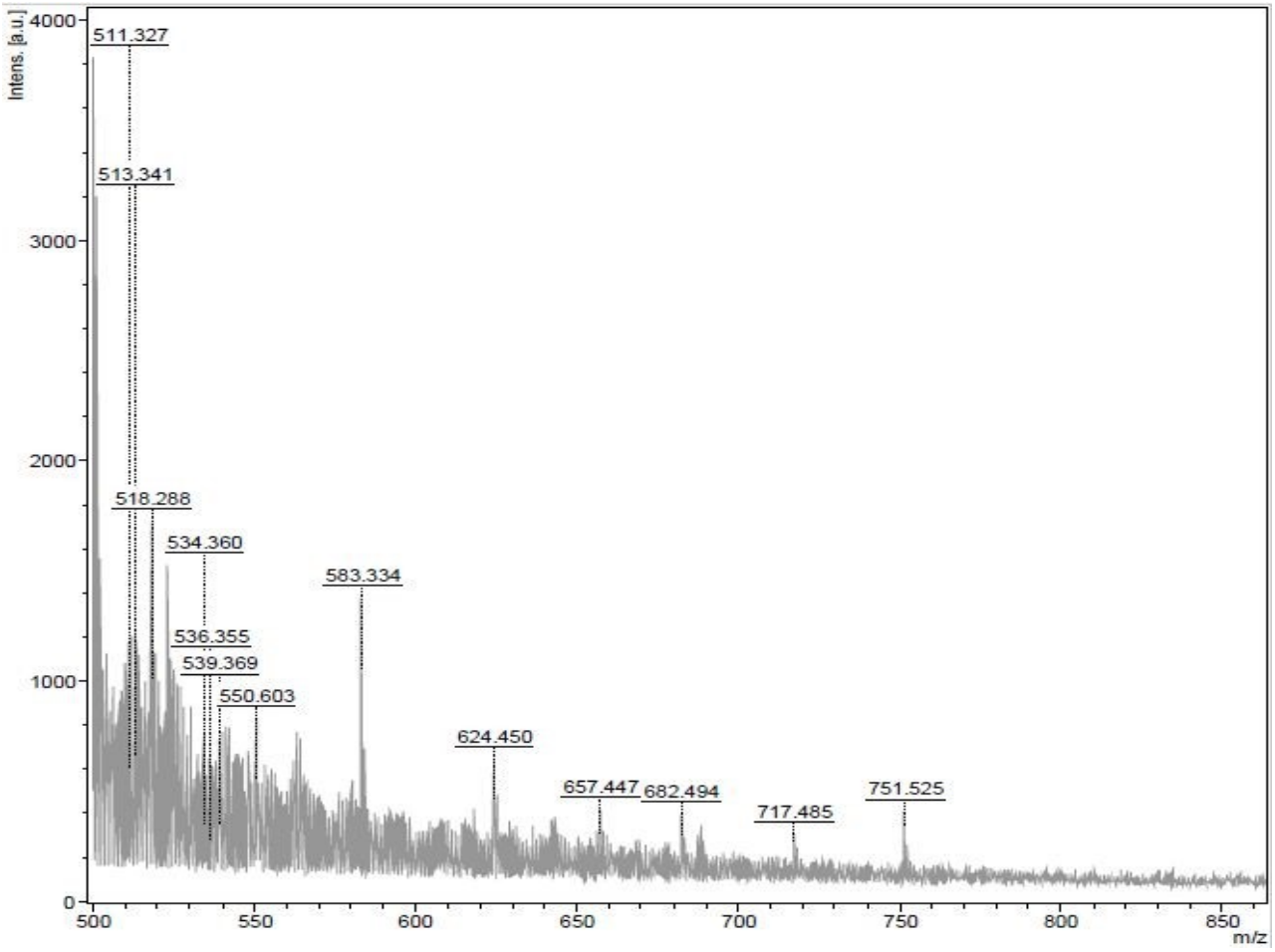

Figure S16. MALDI-TOF spectra of CNP.

Explanation of Peaks based on oxidation scheme[1]

340 + 170 + (4 x 18) + H^+ = 583
340 + 176 + (6 x 18) = 624
308 + 176 + 172 + H^+ = 657
340 + (2 x 170) + $2H^+$ = 682
340 + 178 + 176 + Na^+ = 717
340 + 178 + 176 + 18 + K^+ = 751

18 is mass of H_2O

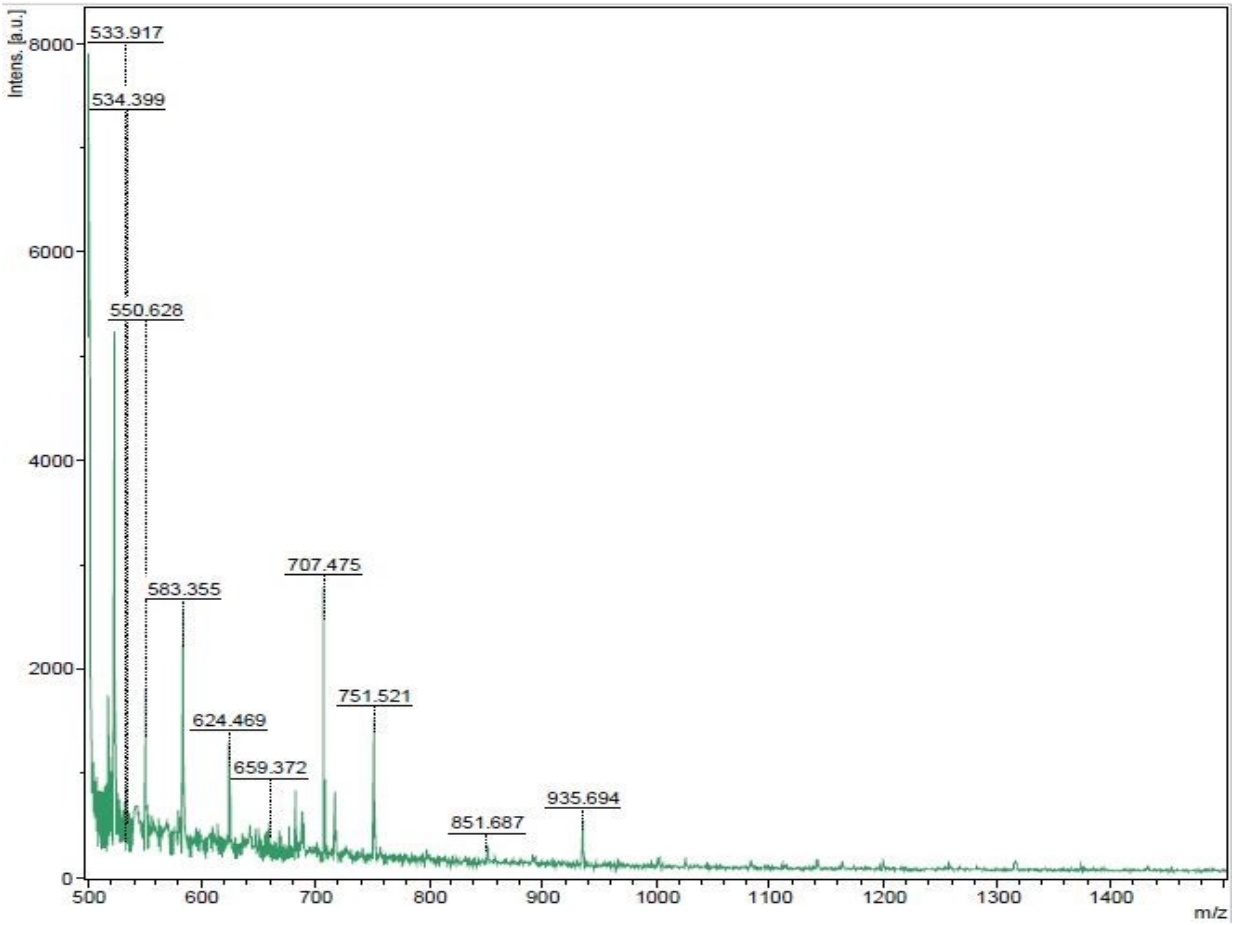

Figure S17. MALDI-TOF spectra of CNP-PS.

Explanation of peaks:

290 + 172 + 119 + $2H^+$ = 583
290 + 176 + 119 + K^+ = 624
290 + 174 + 172 + Na^+ = 659
290 + 178 + (2 x 119) + H^+ = 707
(290 x 2) + 170 + H^+ = 751
290 + (2 x 180) + 178 + Na^+ = 851
(2 x 290) + 178 + 176 + H^+ = 935

119 is mass of 4-vinylaniline

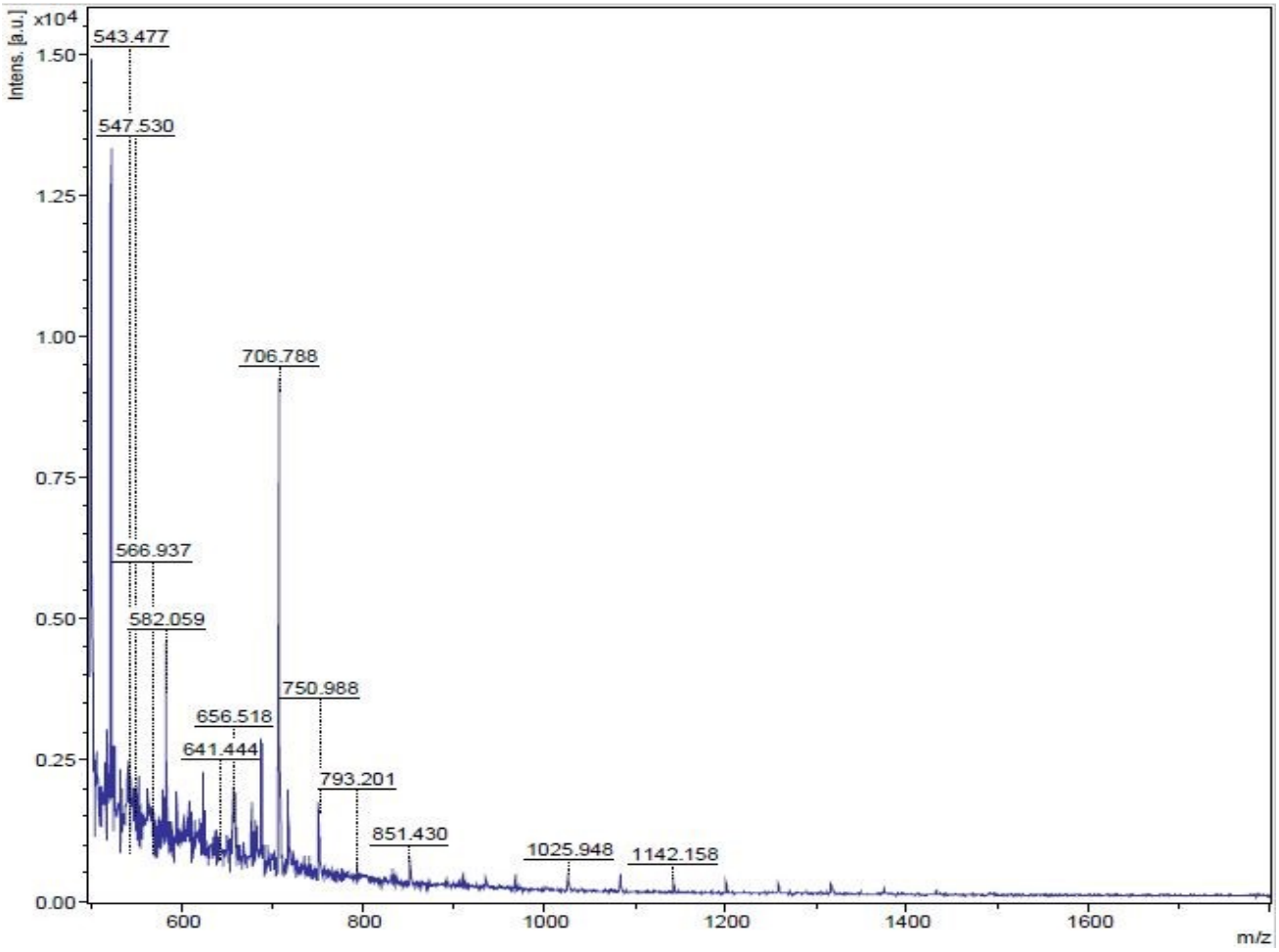

Figure S18. MALDI-TOF spectra of CNP-PS irradiated with UV light for 24h.

Explanation of peaks:

290 + (2 x 145) + $2H^+$ = 582
170 + (2 x 161) + 146 + $3H^+$ = 641
(2 x 174) + 161 + 145 + $2H^+$ = 656
(3 x 174) + 161 + Na^+ = 706
171 + (4 x 145) =751
178 + (2 x 161) + (2 x 145) + $3H^+$ = 793
(3 x 180) + 161 + 146 + $3H^+$ = 851
170 + (4 x 161) + 146 + $7H^+$ = 967
180 + 178 + 176 + (2 x 161) + 146 + Na^+ = 1025
176 + (4 x 146) + (2 x 161) + 2 H^+ = 1084
(2 x 176) + 174 + (2 x 161) + (2 x 146) + $2H^+$ = 1142

Table S1. Time-resolved photoluminescence spectra were acquired and different distribution parameters of the fitted exponential function and intensity average lifetimes ($\tau_{avg.}$) were provided. Excitation wavelength for TRPL experiments were kept to 390nm.

Samples	a_1 (%)	a_2 (%)	t_1 (ns)	t_2 (ns)	$\zeta_{avg.}$	$\chi 2$
CNP	67.78	32.21	0.234	1.897	1.55	1.09
CNP-PS	71.7	28.28	0.169	1.41	1.127	2.3
CNP-PS + UV	75.54	24.45	0.145	2.271	1.94	1.8

Table S2. Quantum yield measurements of different samples using Quinine Sulfate as reference.

Samples	Refractive Index	Quantum Yield
Quinine sulfate	1.33	54.6%
CNP	1.4459	9.2%
CNP-S	1.4459	3.9%
CNP-PS + UV	1.3586	2.6%

Table S3. LDA classification results demonstrating 100% of original grouped cases being correctly classified.

Actual Group	Predicted Group								
	Fe3+	Cu2+	Pb2+	Gd2+	Ru2+	Pr2+	Ca2+	Mn2+	Total
Fe3+	3	0	0	0	0	0	0	0	3
Cu2+	0	3	0	0	0	0	0	0	3
Pb2+	0	0	3	0	0	0	0	0	3
Gd2+	0	0	0	3	0	0	0	0	3
Ru2+	0	0	0	0	3	0	0	0	3
Pr2+	0	0	0	0	0	3	0	0	3
Ca2+	0	0	0	0	0	0	3	0	3
Mn2+	0	0	0	0	0	0	0	3	3

Reference

1. Srivastava, I., Sar, D., Mukherjee, P., Schwartz-Duval, A. S., Huang, Z., Jaramillo, C., Civantos, A., Tripathi, I., Allain, J. P., Bhargava, R., Pan, D. *Nanoscale* **2019**, *11*, 8226.